Structural Basis of Light Harvesting by Carotenoids: Peridinin-Chlorophyll-Protein from *Amphidinium carterae*

Eckhard Hofmann, Pamela M. Wrench, Frank P. Sharples, Roger G. Hiller, Wolfram Welte,* Kay Diederichs

Peridinin-chlorophyll-protein, a water-soluble light-harvesting complex that has a blue-green absorbing carotenoid as its main pigment, is present in most photosynthetic dinoflagellates. Its high-resolution (2.0 angstrom) x-ray structure reveals a noncrystallographic trimer in which each polypeptide contains an unusual jellyroll fold of the α-helical amino- and carboxyl-terminal domains. These domains constitute a scaffold with pseudo-twofold symmetry surrounding a hydrophobic cavity filled by two lipid, eight peridinin, and two chlorophyll *a* molecules. The structural basis for efficient excitonic energy transfer from peridinin to chlorophyll is found in the clustering of peridinins around the chlorophylls at van der Waals distances.

Light-harvesting complexes (LHCs) increase the overall efficiency of photosynthesis by passing absorbed light to reaction centers, where conversion to chemical energy occurs. Photosynthetic dinoflagellates, which make up much of the sea plankton and are the cause of red tides, use about equal amounts of two classes of pigments, carotenoids (*1*) and chlorophyll, for the efficient harvesting of light. Most dinoflagellates have peridinin (Fig. 1) as their predominant carotenoid, enabling them to capture solar energy in the blue-green range (470 to 550 nm), which is inaccessible by chlorophyll alone. In addition to a membrane-bound LHC (*2*), which structurally and functionally resembles that of higher plants (*3*), dinoflagellates have developed a soluble antenna with a high carotenoid:chlorophyll ratio, peridinin-chlorophyll-protein (PCP), that has no sequence similarity with other known proteins (*4*). Variants of PCP with an apoprotein of around 16 kD exist as homodimers (*5*), whereas forms with an apoprotein of around 32 kD probably arose by duplication and fusion of an ancient PCP gene. In PCP from *Amphidinium carterae*, the NH_2- and COOH-terminal domains (*6*) of the cDNA-derived sequence (30.2 kD) share 56% of their residues, and each domain binds a cluster of one chlorophyll *a* and four peridinin molecules. Within each cluster, the efficiency of singlet energy transfer from peridinin to chlorophyll is close to unity (*7*). Models of chromophore interaction within and among the clusters have previously been based on spectroscopic investigations (*7*, *8*). Structural information, such as that available for membrane-bound LHCs from higher plants (*3*) and bacteria (*9*), has greatly enhanced our understanding of antenna systems having chlorophyll as the main pigment. The high-resolution structure of PCP gives insight into the highly organized structural basis of light-harvesting by carotenoids and its efficient transfer to chlorophyll and should be of considerable value for relating theoretical calculations of energy transfer to the experimentally determined spectroscopic parameters.

The crystal structure of PCP from *A. carterae* (*10*) was determined at a resolution of 2.0 Å with the use of x-ray crystallography. Diffraction data and crystallographic procedures are summarized in Table 1. Initial phases at 2.9 Å resolution were obtained by the single isomorphous replacement method and improved by an iterative solvent-flattening and noncrystallographic symmetry-averaging procedure. The resulting electron density map enabled us to trace three crystallographically independent but nearly identical monomers (312 residues) of PCP and to insert the pigments. After extending the resolution to 2.0 Å and refining further, lipids and water molecules were found in difference Fourier maps and were inserted into the model. The lipids are an integral part of the structure; their existence in PCP was unexpected and points to the complexity of the holoprotein assembly. On the basis of well-defined density and possible hydrogen bonds, the lipids were identified (Table 1) as digalactosyl diacyl glycerol (DGDG). We assume that DGDG binds tightly to the chlorophylls before complex formation; its removal during unfolding by acetone may cause the failure of renaturation experiments (*7*). As DGDG is mostly found in the inner thylakoid membrane (*11*), where it is the main lipid, our finding supports the disposition of PCP inside the thylakoid lumen, which was previously based only on an analysis of leader sequences (*4*).

In the crystal structure (Fig. 2), the NH_2- and COOH-terminal halves of the polypeptide form almost identical domains related by a twofold pseudosymmetry axis [root

Table 1. Crystallographic data. Data collection: Native1 and derivative data (5 mM K_2PtCl_4, 1-day soak) were collected on a rotating anode source (CuKα, 40 kV, 100 mA) with a STOE (Darmstadt, Germany) imaging plate detector. Native2 was collected at the BW7B wiggler beamline at DESY on a 30-cm MARresearch (Hamburg, Germany) image plate. All data were processed with XDS (*26*). Phasing: Six heavy-atom binding sites were found using SHELXS (*27*) in Patterson search mode, and four additional sites were found by inspection of difference Fourier maps. Refinement of heavy-atom parameters was done with DAREFI (*28*). The phases could be improved further by inclusion of the anomalous signal and the use of solvent flattening and noncrystallographic symmetry averaging of the trimer in the asymmetric unit (*29*). Model building and refinement: The resulting 2.9 Å electron density map was readily interpretable. An initial model of PCP was built with O (*23*). The full sequence could be included, and 10 pigments were modeled. The initial model was refined with X-PLOR (*24*), including simulated annealing, positional refinement, and manual rebuilding against Native1 and later Native2. Strong noncrystallographic symmetry restraints were applied throughout the refinement. ARP (*30*) was used to obtain unbiased atomic positions for well-connected density in the 2.0 Å difference electron-density map. The arrangement of these atoms, together with possible hydrogen-bonding patterns, was consistent with an interpretation as DGDG molecules. After refinement, the DGDG head groups obey good stereochemistry and show no difference density. The current model consists of 6849 protein atoms, 1890 atoms of pigments and lipids, and 416 water atoms, and the R_{cryst} [$= \Sigma_h|F_o - F_c|/\Sigma_h F_o$, where F_o and F_c are the observed and calculated structure factor amplitudes; summation is over all reflections h] in the resolution range 40 to 2 Å is 17.9% for 93,720 reflections [free R (*24*), 20.1% for 2325 reflections]. Stereochemical deviations from target values are 0.012 Å for bond lengths and 1.3° for bond angles. No residues are in disallowed regions of the Ramachandran plot.

Data	Resolution (Å) (highest shell)	Unique reflections	Completeness (%) (highest shell)	R_{sym}* (%) (highest shell)	R_{iso}† (%)
Native1	2.9 (3.16–2.9)	31362	93.6 (82.4)	8.3 (26.5)	—
Native2	2.0 (2.10–2.0)	96045	92.5 (92.6)	5.4 (19.0)	—
K_2PtCl_4	2.9 (3.16–2.9)	31384	93.6 (58.6)	11.9 (41.1)	33.4

*$R_{sym} = \Sigma_h \Sigma_i|I_{h,i} - \langle I_h\rangle|/\Sigma_h \Sigma_i I_{h,i}$, where $\langle I_h\rangle$ is the mean intensity of all observations of the unique reflection h. †$R_{iso} = \Sigma_h|I_P - I_{PH}|/\Sigma_h(I_P + I_{PH})/2$, where I_P and I_{PH} are the intensities of the native and derivative data sets, respectively; summation is over all reflections h present in both.

E. Hofmann, W. Welte, K. Diederichs, Fakultät für Biologie, Universität Konstanz, Postfach 5560 (M656), 78434 Konstanz, Germany.
P. M. Wrench, F. P. Sharples, R. G. Hiller, School of Biological Sciences, Macquarie University, New South Wales 2109, Australia.
*To whom correspondence should be addressed. E-mail: Wolfram.Welte@uni-konstanz.de

mean square deviation of 0.9 Å (*12*)]. Each domain consists of eight helices (N1 through N8 and C1 through C8) and their intervening loops, with a topology resembling a wide open, right-handed "jellyroll" (*13*); a short β-hairpin loop forms the tip of the jellyroll. The juxtaposition of these domains generates a central, hydrophobic space of about 23 Å by 23 Å by 53 Å filled with the pigments and lipids (holoprotein molecular weight, 38.1 kD). This jellyroll fold has not previously been reported (*14*) for an α-helical protein. The fold appears to be advantageous, as it economizes on the number, size, and angular range of movements during folding of the protein around the chromophores after translocation through the chloroplast membranes. The shape of the protein, with its triangular cross section, can best be described by analogy with a ship, whose bow, sides, stern, and deck are formed by helices. This analogy can be extended to describe the long (40 Å) connection (*12*) between the NH_2- and COOH-terminal domains as the keel of the ship and the chromophores in the interior of the ship as the cargo. Two large openings are found near the bow and the stern, between helices N8 and N6 and between C8 and C6, and two smaller ones are found in the deck, between helices N2 and N7 and between C2 and C7. These openings are filled by the hydrophilic epoxycyclohexane rings of the peridinins (NH_2- and COOH-terminal Per1 to Per4) and the head groups of the lipids.

Monomers of PCP form a noncrystallographic trimer with a diameter of about 100 Å and a thickness of 40 Å; their local twofold axes are tilted by 20° with respect to the trimer plane. Trimerization occurs through mainly hydrophobic interactions of the deck and stern helices and is assisted by hydrogen bonds of the COOH-terminal Per2 epoxycyclohexane ring, which interacts with its symmetry mates around the threefold axis through an intervening water molecule. Trimerization of PCP is consistent with dynamic light-scattering properties of concentrated PCP solutions. Furthermore, we solved by the molecular replacement method two nonisomorphous structures of PCP crystals grown under significantly different conditions and observed the same mode of trimerization in these different environments (*15*). Trimer formation, which is also found in the other two structurally known water-soluble LHCs, bacteriochlorophyll *a* protein (*16*) and phycobiliprotein (*17*), as well as in LHC-II from higher plants (*3*), has been interpreted as advantageous for orienting the pigments and so optimizes the absorption cross section (*16*). It is striking that evolution has used two different structural classes, all-α and all-β, to build the water-soluble PCP and bacteriochlorophyll *a* protein, which have in common a hydrophobic space filled by a cluster of pigments.

In photosynthesis, energy is transferred (*18*) among similar or identical chromophores by two mechanisms. Long-range (up to 100 Å) Förster dipole-dipole interaction depends strongly on the mutual orientation of the dipoles: it is most efficient if dipoles are parallel and end-to-end but is still favorable if they are parallel and side-by-side. Coupling of delocalized excitons occurs at distances of less than 20 Å. For a high efficiency of excitonic energy transfer between carotenoids and chlorophyll, much shorter distances are required, because of the short half-life of the carotenoid excited state (*19*). Circular dichroism studies of PCP (*7*) suggested two chlorophyll-peridinin clusters in which each chlorophyll is arranged between two pairs of mutually orthogonal peridinins. The crystal structure confirms the existence of a NH_2-terminal (Fig. 3) and a COOH-terminal pigment cluster, related by the same local twofold symmetry as is the apoprotein. Each cluster has two pairs of peridinins (Per1-Per2 and Per3-Per4) surrounding a chlorophyll; with-

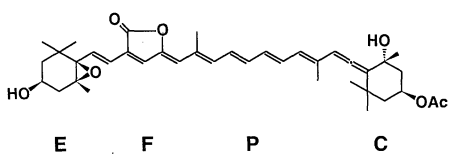

Fig. 1. Structure of peridinin, an asymmetric carotenoid composed of an epoxycyclohexane ring (E) and a polyene chain (P) with a furanic ring (F) and a cyclohexane ring (C). Distortions of the all-trans configuration, as well as contacts of P and F with polar atoms of the protein environment, modify the spectroscopic properties [peridinin in ethanol, absorption maximum λ_{max} = 470 nm (*7*); peridinin in peridinin-chlorophyll-protein (PCP), λ_{max} = 478 nm].

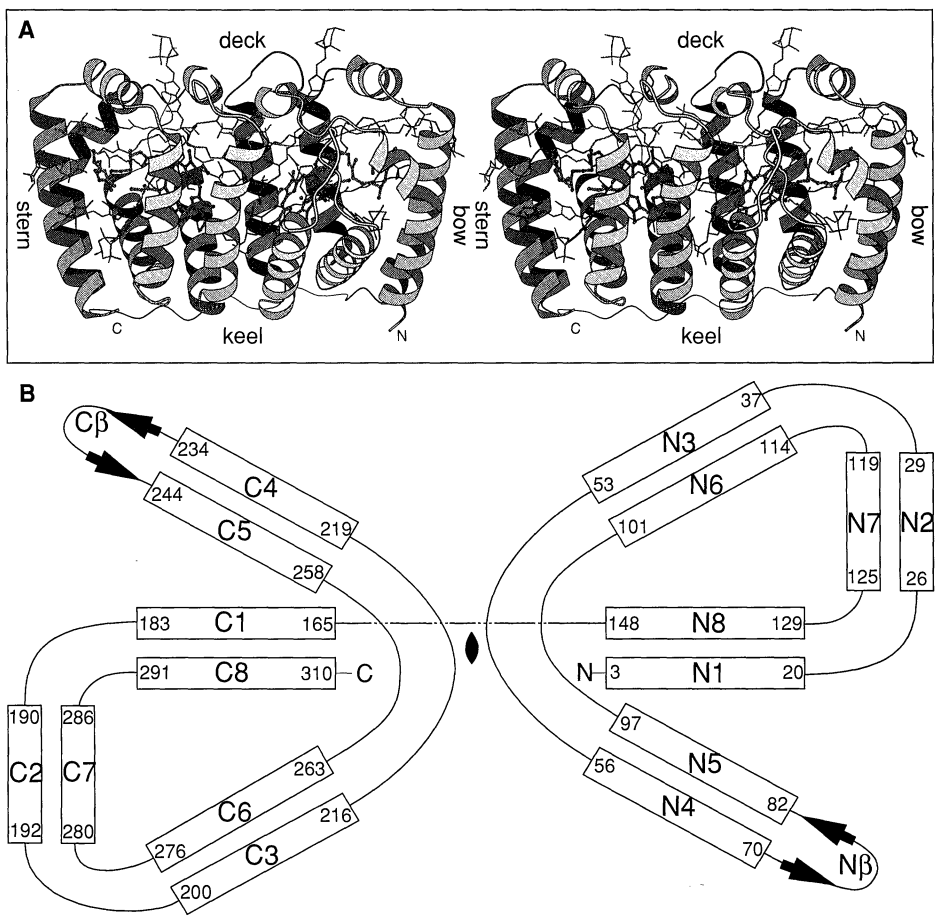

Fig. 2. Structure of PCP. (**A**) Stereo ribbon diagram of a monomer of the PCP complex. The NH_2 terminus is positioned at the lower right of the diagram, the COOH terminus at the lower left. Helices are gray, chlorophyll molecules are green, peridinins are in shades of red (Per1, lightest, to Per4, darkest), and lipids are in blue. The helices form a scaffold resembling a ship, whose parts are labeled. The view is approximately along the trimer axis, and the local twofold pseudosymmetry axis, which relates the NH_2- and COOH-terminal domains, is vertical. [Produced by MOLSCRIPT (*25*).] (**B**) Topology diagram of a PCP monomer. The jellyroll formed by the helices of each domain is depicted in a nonstandard (*13*) way, with NH_2 and COOH termini in the center, thereby conserving the spatial relations between helices. The "ship" consists of the bow (N1 and N8), sides (N3 through N6 and C3 through C6), stern (C1 and C8), and deck (N2, N7, C2, and C7). Helices parallel in the diagram are almost parallel in the structure, whereas all other pairs of adjacent helices cross at angles of around 30° to 50°.

in each pair, closest distances of the polyene chains are less than 4 Å. All peridinins are in an extended all-trans conformation and show small distortions from their average geometry (*20*), which mainly result from interaction with the protein environment. In contrast to the predictions (*7*), the crossing angle within each pair is about 56° (±6°), the furanic rings of the peridinins are close to each other within each pair, and the distance between the centers of mass, which was estimated at 12 Å (*7*), is 5.5 Å (Per1-Per2) and 8.4 Å (Per3-Per4), respectively. Per1 and Per3 are parallel, to within 5°, and flank the tetrapyrrole system on opposite sides, extending a plane that is tilted by 30° from that of chlorophyll (Fig. 3). The other members of each pair, Per2 and Per4, are stacked on opposite faces of the chlorophyll macrocycle and are within 25° of the Q_x and Q_y transition moments (*21*) of chlorophyll, respectively. The conjugated regions of all peridinins are in van der Waals contact (3.3 to 3.8 Å) with the tetrapyrrole ring of chlorophyll, allowing efficient excitonic energy transfer from each peridinin to chlorophyll.

The chlorophylls are completely buried in a hydrophobic environment: half of their surface area is covered by the peridinins, and the remainder is covered by the protein (one-third) and the fatty acid chains (one-sixth) of the lipids. The closest protein-chlorophyll contacts occur through a stacking at van der Waals distance of the imidazole rings of two conserved His residues, His^{66} and His^{229}, onto the tetrapyrrole C ring of the NH_2- and COOH-terminal chlorophylls, respectively. A water molecule, which is on one side hydrogen bonded to these residues, provides the fifth coordination site (distance, 2.0 Å) of the central Mg atoms (Fig. 4). In both clusters, chlorophyll intercalates into the pocket between the two pairs of peridinins, with its phytyl chain projecting into the space between Per1 and Per3. Unlike the situation in LH2 (*9*), where excitonic energy transfer between adjacent chlorophylls takes place, the geometry in PCP allows only Förster energy transfer between chlorophylls of each monomer (distance, 17.4 Å). Distances between chlorophylls of different subunits within a trimer are in the 40 to 55 Å range. The COOH-terminal chlorophylls appear to be oriented most suitably for Förster exchange of excitation energy between the subunits of a trimer (Fig. 5), as their Q_y transition moments are approximately parallel to the trimer axis (inclination, 25°), and their distance (44 Å) is well within the range of dipole-dipole interactions.

The polypeptide chain of PCP serves three main purposes: (i) to provide a hydrophobic environment for the pigments, which would otherwise be insoluble in the aqueous compartment of the chloroplast, (ii) to tune the absorption properties of the pigments, and (iii) to arrange the pigments such that there is efficient energy transfer among them and toward the other components of the photosynthetic apparatus. PCP shares the latter two requirements with the membrane-bound LHC. The structure of LHC-II from higher plants has been elucidated by electron microscopy (*3*) and can serve as a structural model for other LHCs, including that of dinoflagellates, with which it shares about 30% sequence homology (*2*). Interestingly, we note structural similarities that parallel the functional similarities between these two proteins: Both are elongated monomers that associate to form flat trimers, and the trimer interface is in both cases provided primarily by one of the two monomer halves that is related to the other half by a local twofold axis. In a model based on fluorescence rise times, it is

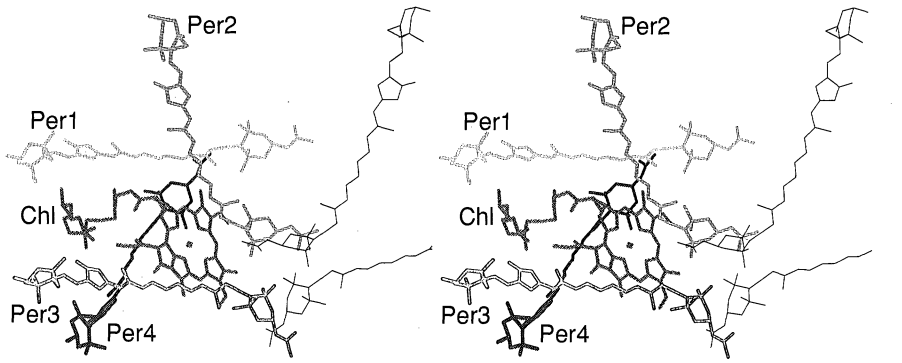

Fig. 3. Stereo view of the arrangement of peridinins and chlorophyll in the NH_2-terminal cluster (heavy lines). Peridinins are labeled Per1 to Per4. Two peridinins (Per2 and Per3) of the COOH-terminal pigment cluster are shown in black (thin lines). The view is the same as in Fig. 2A.

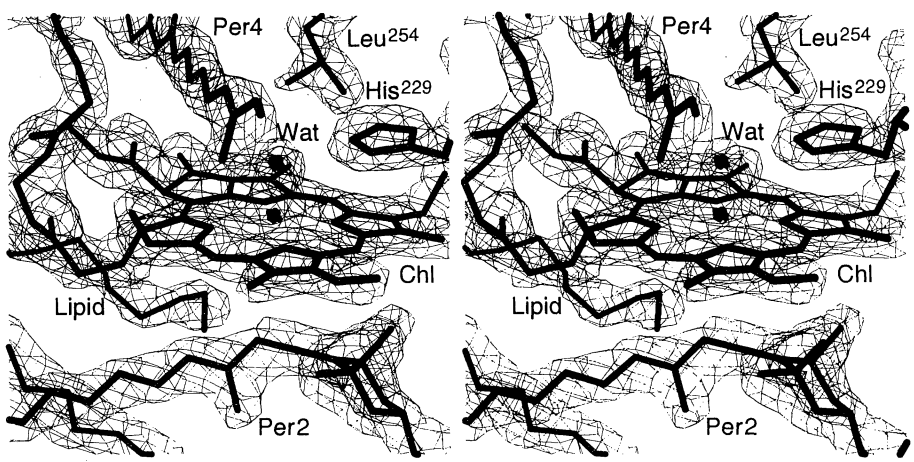

Fig. 4. Electron density map (coefficients $2F_o - F_c$, contoured at 1.5σ) showing a stereo view of the environment of the COOH-terminal chlorophyll (Chl), including Leu^{254}, His^{229}, and parts of Per2, Per4, and one lipid molecule. A water molecule (Wat), which provides the fifth coordination site of the Mg, is also shown. The view is parallel to the trimer axis.

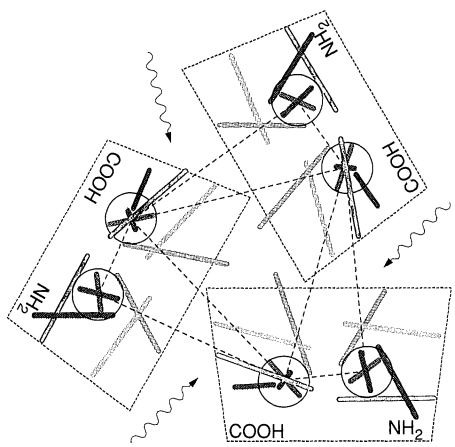

Fig. 5. Model of energy flow to, from, and within the PCP trimer (top view). Light absorbed by the polyene chains of peridinin (red; color-coded as in Fig. 2A) is transferred by an excitonic mechanism to chlorophyll (circled). Crosses represent the transition moments (Q_x, light green; Q_y, dark green). Energy can be equilibrated (dashed lines) among the chlorophylls of the trimer or passed to membrane-bound chlorophylls (below or above the plane of the trimer) by a dipole-dipole mechanism. Individual monomers are delineated by dotted lines, and the NH_2 and COOH termini are indicated.

proposed (*22*) that PCP passes energy from its chlorophylls to those of the membrane-bound LHC. Although the data (*22*) do not exclude direct energy transfer to the core of photosystem 2, the similar appearance of the PCP trimer and that of the intrinsic chlorophyll-carotenoid protein suggests that PCP and LHC could coexist in a stacked configuration. With this proposed geometry, highly efficient Förster energy transfer from PCP to LHC can be expected, because the tetrapyrrole rings of their chlorophylls would be approximately coplanar.

REFERENCES AND NOTES

1. For recent reviews about the photoprotective and light-harvesting functions of carotenoids, see H. A. Frank and R. J. Cogdell, in *Carotenoids in Photosynthesis*, A. Young and G. Britton, Eds. (Chapman & Hall, London, 1993); Y. Koyama, M. Kuki, P. O. Andersson, T. Gillbro, *Photochem. Photobiol.* **63**, 243 (1996).
2. R. G. Hiller, P. M. Wrench, A. A. Gooley, G. Shoebridge, J. Breton, *Photochem. Photobiol.* **57**, 125 (1993); R. Iglesias-Prieto, N. S. Govind, R. K. Trench, *Philos. Trans. R. Soc. London Ser. B* **403**, 381 (1993); R. G. Hiller, P. M. Wrench, F. P. Sharples, *FEBS Lett.* **363**, 175 (1995).
3. W. Kühlbrandt and D. N. Wang, *Nature* **350**, 130 (1991); ——— and Y. Fujioshi, *ibid.* **367**, 614 (1994).
4. B. J. Norris and D. J. Miller, *Plant Mol. Biol.* **24**, 673 (1994).
5. F. T. Haxo, J. H. Kycia, G. F. Somers, A. Bennett, H. W. Siegelman, *Plant Physiol.* **57**, 297 (1976); B. B. Prezelin, in *The Biology of Dinoflagellates*, F. J. R. Taylor, Ed. (Blackwell Scientific, Oxford, 1987), p. 174; R. Iglesias-Prieto, N. S. Govind, R. K. Trench, *Proc. R. Soc. London Ser. B* **246**, 275 (1991); E. L. Triplett *et al.*, *Mol. Mar. Biol. Biotechnol.* **2**, 246 (1993).
6. R. G. Hiller, P. M. Wrench, F. P. Sharples, in *Photosynthesis: From Light to Biosphere*, P. Mathis, Ed. (Kluwer, Dordrecht, Netherlands, 1995), vol. 1, p. 24.
7. P. S. Song, P. Koka, B. B. Prezelin, F. T. Haxo, *Biochemistry* **15**, 4422 (1976); P. Koka and P. S. Song, *Biochim. Biophys. Acta* **495**, 220 (1977).
8. D. Carbonera, G. Giacometti, G. Agostini, *Spectrochim. Acta A* **51**, 115 (1995).
9. G. McDermott *et al.*, *Nature* **374**, 517 (1995).
10. Purification and crystallization: *A. carterae* was cultivated as reported previously (*2*), and PCP was purified from a water-soluble algal extract by size-exclusion chromatography and chromatofocusing. Crystals grew in the monoclinic space group *C*2 with cell dimensions of $a = 198.4$ Å, $b = 116.3$ Å, $c = 67.0$ Å, and $\beta = 94.9°$. PCP is present as a trimer with an overall weight-average molecular weight of 114 kD in the asymmetric unit. The absorption spectrum is unchanged by the crystallization process. PCP crystals were grown at 17°C in hanging drops containing 5 mg of protein per milliliter, 4 to 6% PEG8000 (PEG, polyethylene glycol) in the crystallization buffer [100 mM $MgCl_2$, 50 mM KCl, 24 mM triethylammoniumphosphate buffer, and 50 mM tris-HCl (pH 5.8) or 100 mM $MgCl_2$, 50 mM KCl, and 25 mM MES-KOH (pH 5.8)] with a reservoir of 8 to 12% PEG8000. For heavy-atom screening, crystals were transferred to droplets of equivalent PEG concentration in MES crystallization buffer containing the heavy-atom compound.
11. A. Rawlyer, M. Meylan-Bettex, P. A. Siegenthaler, *Biochim. Biophys. Acta* **1233**, 122 (1995).
12. Using a distance cutoff of 3.8 Å in the program O (*23*), we aligned 149 C_α atom pairs. Residues 151 through 163 are in extended conformation and connect the NH_2- and COOH-terminal halves; consequently, they do not obey twofold local symmetry.
13. J. Richardson, *Adv. Protein Chem.* **34**, 167 (1981).
14. Structural comparisons against databases of unique structures were performed with two different programs: DALI [L. Holm and C. Sander, *J. Mol. Biol.* **233**, 123 (1993)] and SUPERIMPOSE [K. Diederichs, *Proteins Struct. Funct. Genet.* **23**, 187 (1995)].
15. These two other crystal forms of PCP were obtained by a different purification scheme involving ammonium sulfate precipitation [K. Steck, T. Wacker, W. Welte, F. P. Sharples, R. G. Hiller, *FEBS Lett.* **268**, 48 (1990)]. Data for space group *P*1 were collected to 2.7 Å resolution from one crystal on a RAXIS IIc image plate detector at Molecular Structure Corporation (Houston, TX). Data for space group *C*2 with cell axes different from (*10*) were measured from one crystal on a FAST area detector at CNRS (Grenoble, France) to a maximum resolution of 3.2 Å. The crystal structures were solved by the molecular replacement procedures as implemented in the program X-PLOR (*24*). In both cases, we used a trimer of PCP as the search model and obtained unambiguous solutions of the rotation and translation functions. After rigid body refinement, the *R* factor was less than 30% for both crystal forms. The correctness of the molecular replacement solutions was confirmed by omit maps showing the chlorophyll molecules, which had been left out of the model used for structure factor calculation.
16. B. W. Matthews, R. E. Fenna, M. C. Bolognesi, M. F. Schmid, J. M. Olson, *J. Mol. Biol.* **131**, 259 (1979).
17. T. Schirmer, W. Bode, R. Huber, W. Sidler, H. J. Zuber, *ibid.* **184**, 257 (1985).
18. For a review, see T. Förster, in *Modern Quantum Chemistry, Istanbul Lectures, Part III: Action of Light and Organic Crystals*, O. Sinanoglu, Ed. (Academic Press, New York, 1965), pp. 93.
19. Estimates of distances permitting efficient energy transfer from peridinins to chlorophyll were given as at most 5.8 to 8.6 Å (*7*), approximately 5.0 Å (*22*), and 4.5 Å [T. Gillbro *et al.*, *Photochem. Photobiol.* **57**, 44 (1993)].
20. Pairwise comparisons give root-mean-squares deviations between 0.6 and 1.3 Å.
21. The direction of the Q_y transition moment was taken as the vector between the C1B and C2D atoms of the porphyrin ring [nomenclature as in D. E. Tronrud, M. F. Schmid, B. W. Matthews, *J. Mol. Biol.* **188**, 443 (1986)].
22. M. Mimuro, N. Tamai, T. Ishimaru, I. Yamazaki, *Biochim. Biophys. Acta* **1016**, 280 (1990).
23. T. A. Jones, J. Y. Zou, S. W. Cowan, M. Kjeldgaard, *Acta Crystallogr. A* **47**, 110 (1991).
24. A. T. Brünger, *X-PLOR Version 3.1* (Yale Univ. Press, New Haven, CT, 1987); *Nature* **355**, 472 (1992).
25. P. Kraulis, *J. Appl. Crystallogr.* **24**, 946 (1991).
26. W. Kabsch, *ibid.* **21**, 916 (1988).
27. G. M. Sheldrick, *Acta Crystallogr. A* **46**, 467 (1990).
28. R. E. Dickerson, J. E. Weinzierl, R. A. Palmer, *Acta Crystallogr. B* **24**, 997 (1968); K. Diederichs, *Jt. CCP4 ESF-EACBM Newsl. Protein Crystallogr.* **31**, 23 (1994).
29. W. Furey and S. Swaminathan, in *Methods Enzymol.*, in press.
30. V. S. Lamzin and K. S. Wilson, *Acta Crystallogr. D* **49**, 127 (1993).

31. We thank the staff of the European Molecular Biology Laboratory at the Deutsches Elektronen-Synchrotron (DESY) (Hamburg, Germany) for help during synchrotron data collection and the staff of Molecular Structure Corporation (Houston, TX) for the opportunity to collect x-ray data of a *P*1 crystal during a demonstration. We also thank K. Steck and P. Timmins for help in the early stages of the project, P. A. Karplus for comments on the manuscript, and W. Kreutz for support. This work was supported by grants from the Deutsche Forschungsgemeinschaft and the Australian Research Council. The atomic coordinates have been submitted to the Brookhaven protein database (ID code 1PPR).

11 March 1996; accepted 23 April 1996

Neural Substrates for the Effects of Rehabilitative Training on Motor Recovery After Ischemic Infarct

Randolph J. Nudo,* Birute M. Wise, Frank SiFuentes, Garrett W. Milliken†

Substantial functional reorganization takes place in the motor cortex of adult primates after a focal ischemic infarct, as might occur in stroke. A subtotal lesion confined to a small portion of the representation of one hand was previously shown to result in a further loss of hand territory in the adjacent, undamaged cortex of adult squirrel monkeys. In the present study, retraining of skilled hand use after similar infarcts resulted in prevention of the loss of hand territory adjacent to the infarct. In some instances, the hand representations expanded into regions formerly occupied by representations of the elbow and shoulder. Functional reorganization in the undamaged motor cortex was accompanied by behavioral recovery of skilled hand function. These results suggest that, after local damage to the motor cortex, rehabilitative training can shape subsequent reorganization in the adjacent intact cortex, and that the undamaged motor cortex may play an important role in motor recovery.

The motor cortex is thought to be important in the initiation of voluntary motor actions, especially those associated with fine manipulative abilities. Thus, a stroke or other injury to the motor cortex results in weakness and paralysis in the contralateral musculature and disruption of skilled limb use (*1*). However, a gradual return of some motor abilities often occurs in the weeks and months after injury (*2*). At least in humans, complete recovery of function in distal musculature, including independent control of digits, is rare (*3*).

Neurophysiological and neuroanatomical bases have been sought to account for functional motor recovery after cortical injury. It is assumed that other parts of the motor system must "take over" the func-